environmental
microbiology

Environmental Microbiology (2018) **20**(1), 385–401 doi:10.1111/1462-2920.14014

Multiplex quantitative SILAC for analysis of archaeal proteomes: a case study of oxidative stress responses

**Lana J. McMillan,[1,2] Sungmin Hwang,[1]
Rawan E. Farah,[1] Jin Koh,[3] Sixue Chen[2,3,4] and
Julie A. Maupin-Furlow[1,2]***
[1] *Department of Microbiology and Cell Science, Institute of Food and Agricultural Sciences, University of Florida, Gainesville, FL 32611, USA.*
[2] *Genetics Institute, University of Florida, Gainesville, FL 32611, USA.*
[3] *Proteomics and Mass Spectrometry, Interdisciplinary Center for Biotechnology Research, University of Florida, Gainesville, FL 32611, USA.*
[4] *Department of Biology, College of Liberal Arts and Sciences, University of Florida, Gainesville, FL 32611, USA.*

Summary

Stable isotope labelling of amino acids in cell culture (SILAC) is a quantitative proteomic method that can illuminate new pathways used by cells to adapt to different lifestyles and niches. Archaea, while thriving in extreme environments and accounting for ~20%–40% of the Earth's biomass, have not been analyzed with the full potential of SILAC. Here, we report SILAC for quantitative comparison of archaeal proteomes, using *Haloferax volcanii* as a model. A double auxotroph was generated that allowed for complete incorporation of $^{13}C/^{15}N$-lysine and ^{13}C-arginine such that each peptide derived from trypsin digestion was labelled. This strain was found amenable to multiplex SILAC by case study of responses to oxidative stress by hypochlorite. A total of 2565 proteins was identified by LC-MS/MS analysis (q-value ≤ 0.01) that accounted for 64% of the theoretical proteome. Of these, 176 proteins were altered at least 1.5-fold (p-value < 0.05) in abundance during hypochlorite stress. Many of the differential proteins were of unknown function. Those of known function included transcription factor homologs related to oxidative stress by 3D-homology modelling and orthologous group comparisons. Thus, SILAC is found to be an ideal method for quantitative proteomics of archaea that holds promise to unravel gene function.

Received 2 August, 2017; revised 27 November, 2017; accepted 28 November, 2017. *For correspondence. E-mail jmaupin@ufl.edu; Tel. (352) 392-4095; Fax (352) 395-5922.

Introduction

Quantitative proteomics is a valuable tool for investigating protein abundances in cells exposed to different conditions. Two main types of quantitative proteomic methods are used in research: label and label-free (Megger *et al.*, 2014). Labelling methods permit for the direct quantification of proteins and reduce bias between samples by allowing for multiplexing. Label-free methods avoid the expense of labelling but do not allow for the mixing of the different samples into a single pool for uniform processing (Ong *et al.*, 2002; Megger *et al.*, 2014). Proteomic studies that use stable isotope labelling in cell culture (SILAC) yield robust quantitative comparisons and allow for multiplexing (Ong *et al.*, 2002). SILAC relies upon the incorporation of 'light' (unlabelled) compared to 'heavy' amino acids (labelled with isotopes such as ^{13}C, ^{15}N, ^{2}H and ^{18}O) into the proteome during cell culture (Ong *et al.*, 2002; Ong and Mann, 2006). SILAC is best performed when the heavy amino acids are essential for growth as seen for study of bacteria and eukaryotes (Ong and Mann, 2006). If essential, the externally added heavy amino acids are fully incorporated into the proteome after several cell doublings and can be used for comparison to cells grown with light amino acids.

Archaea are ideal for study of the mechanisms used by cells to withstand harsh environmental conditions, as many archaea thrive in extreme niches, such as hydrothermal vents, acidic hot springs and hypersaline lakes (Pedone *et al.*, 2004; Bidle *et al.*, 2008; Kort *et al.*, 2013). Archaeal proteomes have been analyzed quantitatively by use of isobaric tags for relative and absolute quantitation (iTRAQ), isotope-coded protein label (ICPL) and label-free methods [e.g., (Xia *et al.*, 2006; Kirkland *et al.*, 2008; Van *et al.*, 2008; Humbard *et al.*, 2009; Tebbe *et al.*, 2009; Williams *et al.*, 2011; Kort *et al.*, 2013; Cerletti *et al.*, 2015)]. However, archaeal proteomes have yet to be analyzed by the preferred method of multiplex SILAC using strains that require arginine and lysine for growth. The advantage of this latter approach is that the proteomes can be completely labelled with heavy (vs. light) arginine and lysine. These fully labelled proteomes are amenable to multiplexing and subsequent digestion with trypsin, a serine protease that cleaves carboxyl to lysine and arginine residues. This approach allows for the theoretical labelling of each tryptic peptide generated from the proteome and, thus, enhances the sensitivity of identification and quantification of proteins by a multiplexed SILAC approach.

Here, we report the generation of a SILAC-compatible strain of *Haloferax volcanii* and use SILAC to investigate differential protein abundance during oxidative stress in this archaeon, originally isolated from the Dead Sea. To our knowledge, such a SILAC-based study that demonstrates complete labelling and quantitative comparison of archaeal proteomes using heavy (vs. light) arginine and lysine has not been previously reported. Our focus was on oxidative stress, often encountered by halophilic archaea in hypersaline environments that undergo cycles of desiccation and intense ultraviolet (UV) radiation resulting in the generation of reactive oxygen species (ROS) (Jones and Baxter, 2017). Our findings advance multiplex SILAC analysis of archaeal proteomes while providing an insight into the responses of archaea to oxidative stress at the proteome level.

Results and discussion

Generation of an Hfx. volcanii SILAC compatible double auxotroph

Hfx. volcanii H26, a pHV2^{-} Δ*pyrE2* derivative of DS2 (Allers *et al*., 2010), can biosynthesize all 20 standard amino acids when cultured in minimal medium and, thus, is not compatible for study by SILAC. To overcome this limitation, the pathways of lysine and arginine biosynthesis were targeted for deletion by homologous recombination. The rationale for generating this mutant strain was that the proteins analyzed by LC-MS/MS would first be enzymatically digested into peptides using trypsin, a serine protease which cuts carboxyl to lysine and arginine residues. Thus, growth of the *Hfx. volcanii* double auxotroph for lysine and arginine in medium supplemented with heavy lysine and arginine would theoretically label each tryptic peptide and allow for robust identification and quantification of proteins by a multiplexed SILAC approach.

To predict the best gene candidates for generating an *Hfx. volcanii* double auxotroph for lysine and arginine, we relied upon KEGG (Kyoto Encyclopedia of Genes and Genomes) pathway predictions. The *lysA* (diaminopimelate decarboxylase EC 4.1.1.20; HVO_1098) gene homolog was targeted for deletion based on its putative function in synthesis of L-lysine and CO_2 from *meso*-2,6-diaminoheptanedioate. Likewise, the gene homolog of *argH* (argininosuccinate lyase EC 4.3.2.1; HVO_0048) was selected for deletion based on its predicted catalysis of the last step of arginine biosynthesis: the production of L-arginine and fumarate from L-argininosuccinate.

Using a markerless deletion strategy, the *lysA* and *argH* gene homologs were deleted from the *Hfx. volcanii* H26 genome. The mutations were found to confer amino acid auxotrophy. The H26 Δ*lysA* mutant (LM06) was unable to grow on glycerol minimal medium (GMM) unless supplemented with L-lysine (Fig. 1A). The lysine auxotrophy of LM06 was relieved when the *lysA* homolog was ectopically expressed, compared to the empty vector control (Fig. 1A). Similarly, the H26 Δ*argH* mutant (LM07) was unable to grow on GMM unless supplemented with L-arginine and was restored in growth to parental ('wild-type') levels when the *argH* gene homolog was ectopically expressed (Fig. 1B). The double deletion strain LM08 (H26 Δ*argH* Δ*lysA*) was found auxotrophic for both lysine and arginine, with a concentration of 200 μM of each amino acid found sufficient to restore growth of this mutant on GMM (Fig. 2A).

Sodium hypochlorite causes oxidative stress in Hfx. volcanii

Hfx. volcanii was next investigated under conditions of oxidative stress. Reactive oxygen species (ROS) cause damage to biomolecules when their intracellular levels exceed the antioxidant and reducing capabilities of the cell (Cabiscol *et al*., 2000; Shang and Taylor, 2011). Sodium hypochlorite (NaOCl) in solution forms hypochlorous acid (HOCl) which is a potent oxidant that disrupts protein structure and causes irreversible protein aggregation, leading to a loss of function (Salo *et al*., 1990; Shang and Taylor, 2011). Damage by HOCl is not limited to proteins, lipids undergo peroxidation (Panasenko, 1997) and cell walls become more permeable (Sips and Hamers, 1981). Nucleotides also interact with HOCl causing disruption of purine and pyrimidine rings (Dennis *et al*., 1979) and damage to DNA (Takehara *et al*., 1994). Biological systems in environments with high concentrations of chloride are prone to the oxidation of Cl^{-} to hypochlorous acid (HOCl) or a similarly reactive chlorine electrophile (Ortiz-Bermudez *et al*., 2003; Wang, 2016). Thus, *Hfx. volcanii* was examined for its sensitivity to ROS damage by hypochlorite as this microbe thrives in hypersaline environments that have high concentrations of chloride.

The survival rate and protein oxidation state of *Hfx. volcanii* was found to be impaired when log-phase cells were exposed to NaOCl. *Hfx. volcanii* had a survival rate of 63% when treated with 2.5 mM NaOCl for 20 min and plated on GMM agar and did not recover when the NaOCl concentration was increased to 7.5 mM (Fig. 2B). In GMM liquid cultures, *Hfx. volcanii* cells were sensitive, but recovered, from treatment with 2 mM NaOCl (Fig. 2C). By contrast, the cells did not fully recover when treated with 5 mM NaOCl and appeared nonviable at 8–11 mM NaOCl (Fig. 2C), consistent with the observations by plate assay (Fig. 2B). When proteomes are oxidized, cysteine residues form promiscuous disulfide bonds (Pajares *et al*., 2015).

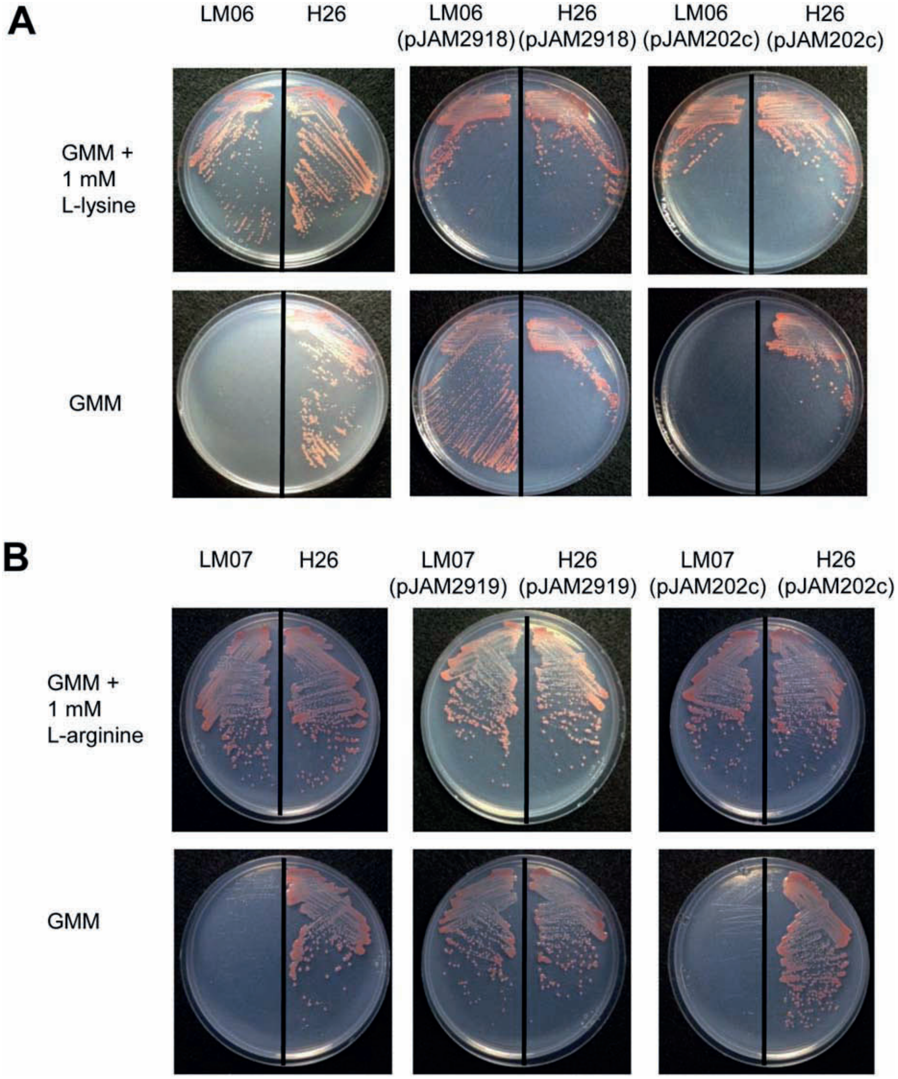

Fig. 1. *Hfx. volcanii* Δ*lysA* and Δ*argH* mutations confer lysine and arginine auxotrophy, respectively.
A. Top row: glycerol minimal medium (GMM) supplemented with 1 mM lysine. Bottom row: GMM alone. Left column, LM06 (H26 Δ*lysA*) was plated with H26 (parent). Center column, LM06 and H26 carry plasmid pJAM2918 for ectopic expression of *lysA*. Right column, LM06 and H26 contain the empty vector, pJAM202c.
B. Top row: GMM supplemented with 1 mM arginine, bottom row: GMM alone. Left column, LM07 (H26 Δ*argH*) was plated with H26 (parent). Center column, LM07 and H26 carry plasmid pJAM2919 for ectopic expression of *argH*. Right column, LM07 and H26 contain the empty vector, pJAM202c. See methods for details. [Colour figure can be viewed at wileyonlinelibrary.com]

Here, a 20 min treatment of cells with 2.5 mM NaOCl was found to decrease (by 63%) the level of free sulfhydryl groups detected in cell lysate by Ellman's reagent, thus, revealing the formation of disulfide bonds in the proteome (Fig. 2D). Based on these results, hypochlorite stress was found to reduce cell viability and stimulate the formation of disulfide bonds in *Hfx. volcanii*.

Two subcultures sufficient for full isotopic incorporation

To achieve full isotopic incorporation of the SILAC amino acids, *Hfx. volcanii* LM08 cells were subcultured twice and allowed to grow for 6.5 doublings in the labelled medium prior to analysis of the proteome by LC-MS/MS. Out of the 3094 peptide groups identified, all had full incorporation of lysine (+8) and arginine (+6). In eukaryotes, [$^{13}C_6$] arginine becomes [$^{13}C_5$] proline through the arginase pathway (Ong *et al*., 2003; Van Hoof *et al*., 2007; Bendall *et al*., 2008). *Hfx. volcanii* has a predicted arginase homolog (EC:3.5.3.1) HVO_1575 (*rocF*), so proline conversion was monitored. Conversion of heavy proline (+5) from arginine occurred 34.3% ± 5.3% of the time from peptides in the top three most abundant proteins (Table 1). While this conversion could cause problems in studies where multiple isotopic forms of arginine are used (Van Hoof *et al*., 2007; Bendall *et al*., 2008; Bicho *et al*., 2010), conversion was not an issue in this study which relied upon the use of one form of heavy arginine coupled with light arginine.

SILAC as an effective method to quantify the differential abundance of proteins in archaea

Using the SILAC method, *Hfx. volcanii* cells were treated with and without 2.5 mM NaOCl for 20 min ($n = 4$). A total of 2565 proteins was identified across all four replicates representing 64% of the theoretical proteome (3996 proteins, Proteome ID: UP000008243) at a FDR adjusted

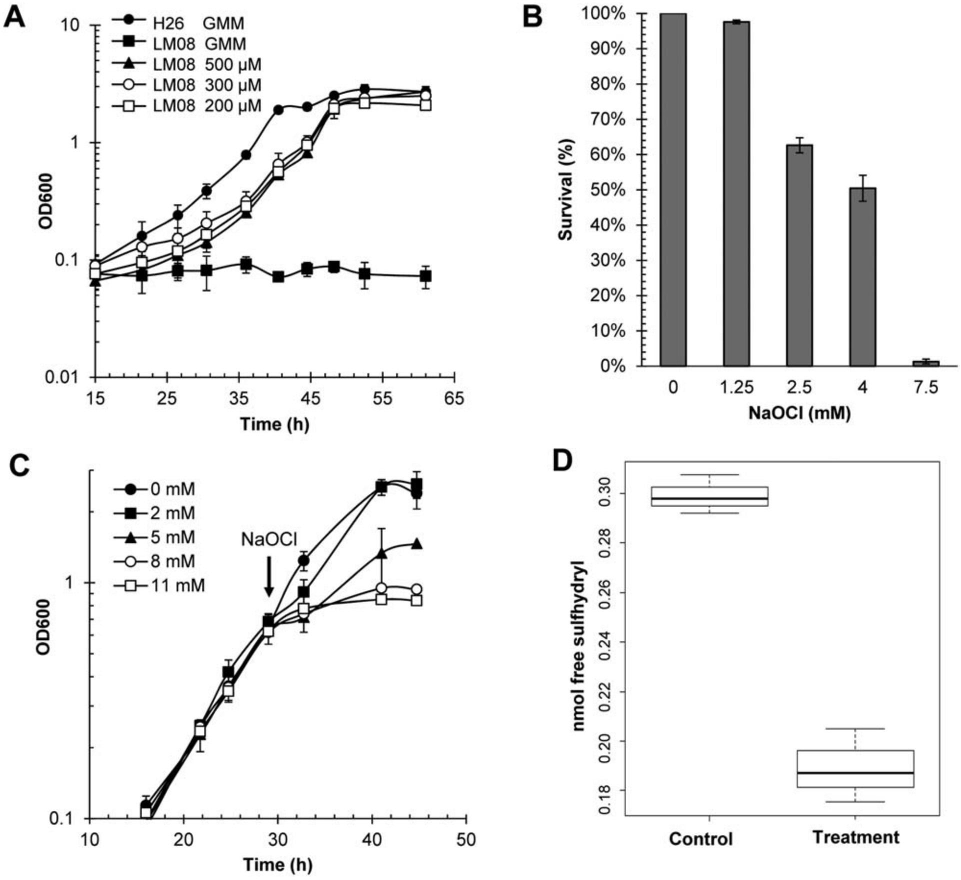

Fig. 2. SILAC ready *Hfx. volcanii* strain and conditions for testing oxidative stress.

A. Growth of the lysine and arginine double auxotroph *Hfx. volcanii* LM08 (H26 Δ*lysA* Δ*argH*) on glycerol minimal medium (GMM) supplemented with lysine and arginine at 0, 200, 300, 500 μM of each. Parent strain (H26) was grown in GMM without lysine or arginine supplementation.

B. Cell survival after NaOCl treatment. H26 cells were grown in GMM to log phase (OD_{600} 0.6–0.9) and treated with 0, 1.25, 2.5, 4 and 7.5 mM NaOCl for 20 min. Treated cells were plated at 10^{-7} dilution on ATCC974 solid medium and individual colony forming units (CFUs) were counted.

C. H26 cells were grown to log phase (OD_{600} 0.6–0.9) in GMM, treated with NaOCl at 0, 2, 5, 8, 11 mM and monitored for growth for a 15 h period after treatment.

D. Ellman's reagent assay for free sulfhydryl groups. LM08 cells were grown in GMM supplemented with 300 μM lysine and 300 μM arginine and treated with 0 mM (control) and 2.5 mM NaOCl for 20 min. Cells were lysed by sonication and total protein was assayed for sulfhydryl content by Ellman's reagent. See methods for details.

p-value (or *q*-value) of 0.01 or less implying that 1% of significant tests will result in false positives (Fig. 3A and Supporting Information Table S2). A total of 1806 proteins was identified ($q\text{-value} \leq 0.01$) in all four replicates. To determine the efficiency of the tryptic digest, the peptides from the top three most abundant proteins by emPAI value were used to count missed cleavages out of total theoretical cleavages. The trypsin digest had a 48.6% mean efficiency and a standard deviation of 8.9%.

The 50 most and least abundant proteins in all four replicates, irrespective of condition were determined by emPAI value and further analyzed for putative function by TMpred and arCOG (Supporting Information Tables S3 and S4). Of the 50 most abundant proteins, 34% (17 proteins) were found to have predicted TM domain(s), 28% (14 proteins) were associated with translation and ribosome structure, 18% (9 proteins) were predicted to function in amino acid transport and metabolism and 16% (8 proteins) were involved in energy production and conversion. Only 6 (12%) of the 50 most abundant proteins were unannotated or of unknown function by arCOG. By contrast, when classified by arCOG, 64% (32 proteins) of the 50 least abundant proteins were of unknown function with five proteins associated with carbohydrate transport and metabolism, three proteins of signal transduction and three proteins of amino acid transport and metabolism. Nearly half (48%) of the least abundant proteins had predicted TM domains. When considering the 50 most and 50 least

Table 1. Heavy proline conversion from heavy arginine.[a]

Replicate	Heavy prolines	Total prolines	Proportion (heavy/total)	Average (heavy/total)	Standard deviation (heavy/total)
1	2640	6580	0.401	0.343	0.053
2	1169	3128	0.374		
3	1211	4131	0.293		
4	1005	3316	0.303		

a. Conversion calculated based on the top three most abundant proteins (UniProt: D4GZY6, D4GXX8 and D4GWB2), as determined by emPAI value. Data used to support these calculations are listed in Supporting Information Table S1.

abundant proteins identified, 41% had predicted TM domains suggesting the coverage of TM domain proteins was well represented, as 24% of the theoretical proteome is predicted to be TM domain proteins (Kirkland *et al*., 2008). Proteins associated with translation are typically abundant (Beck *et al*., 2011), while proteins with TM domains are often underrepresented in proteomic studies (Schrimpf *et al*., 2009). Here, we found proteins associated with translation, protein folding, transport and central metabolism to be highly abundant, while proteins of unknown function to be least abundant in the *Hfx. volcanii* proteome.

When comparing protein abundance among haloarchaea, some interesting findings were noted. Of the 30 proteins determined to be of high abundance in *Halobacterium salinarum* (sp. NRC-1) by 2D-PAGE (Shukla, 2006), the translation elongation factor 1α (HVO_0359, Eef1A), type I glyceraldehyde-3-phosphate dehydrogenase (HVO_0481, GapB), peptidyl-prolyl cis-trans isomerase (HVO_2222, PpiA), a riboflavin/purine nucleoside binding protein (HVO_1401, YufN) (3D structural homolog of PDB:4IIL and 2FQX) and proteins of the ribosome were also found to be of high abundance in *Hfx. volcanii*. However, the hypothetical *N*-acyltransferase (NTRANS_0004) of chromatin remodelling proposed to be one of the most abundant proteins in *Hfx. volcanii* based on transcriptome data (Ammar *et al*., 2012) was not identified at the proteome level in this or previous study (Kirkland *et al*., 2008). NTRANS_0004 transcript maps to the same region of the *Hfx. volcanii* genome (NC_013967.1: 936059–936368) as the signal recognition particle sRNA *ffs* (HVO_RS19635; NC_013967.1:936051–936362). This overlap in transcript sequence combined with the inability to detect NTRANS_0004 at the proteome level suggests the transcript is the noncoding *ffs*.

A label-swap replication of SILAC experiments was used to test the effect of isotope labelling on differential protein abundance. In the NaOCl treatment group, replicates 1 and 3 were labelled with heavy lysine (+8) and heavy arginine (+6), while replicates 2 and 4 were grown with light lysine and arginine. The replicates of the treatment group were inversely correlated. When comparing the control peptide abundance values for the 50 most abundant proteins by emPAI value, only one protein, a putative

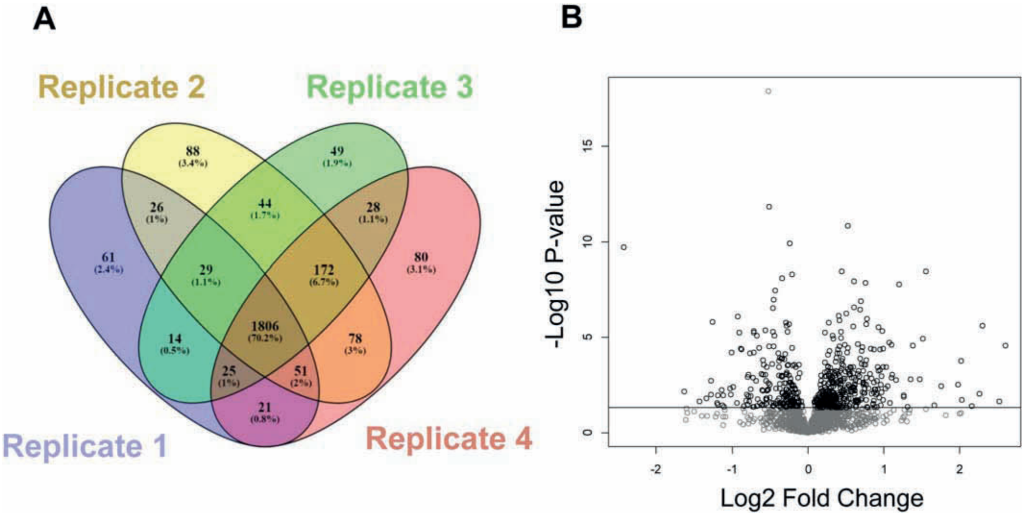

Fig. 3. *Hfx. volcanii* proteins identified by SILAC and found to be of differential abundance during NaOCl-mediated oxidative stress.
A. Venn diagram of proteins identified in each replicate with at least two peptides with a FDR adjusted *p*-value (or *q*-value) of 0.01 or less.
B. Volcano plot of protein abundance values displayed as $\log_2$ of the fold change ratio (NaOCl treatment compared to control) and $-\log_{10}$ of *p*-value. Black points are statistically significant with $p\text{-value} < 0.05$. See methods for details.

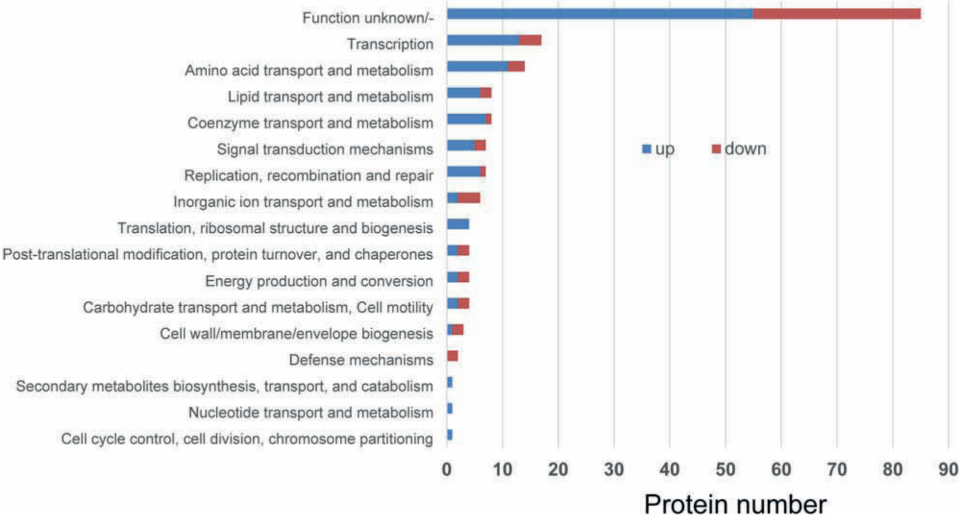

Fig. 4. General classification of the differential proteome of *Hfx. volcanii* identified during oxidative stress. Proteins at least 1.5-fold up (blue) or down (red) in abundance after 20 min treatment with 2.5 mM NaOCl (at a *p*-value of 0.05 or less) were classified by arCOG. See methods for details.

phosphoserine phosphatase (HVO_0880), was detected at a statistically significant fold change in abundance (0.93-fold at a *p*-value < 0.01) that was due to the light/heavy amino acids (Supporting Information Table S5). The abundance of the unlabelled peptides of HVO_0880 were at 92.9% ± SD 5.9% of the same peptides with the lysine (+8) and arginine (+6) labelling. This limited difference observed due to the label swap revealed SILAC had little if any effect on protein abundance in *Hfx. volcanii*. Label swap experiments show SILAC labelling does not disturb peptide abundances between different label states in other organisms (Ong *et al.*, 2002; Butter *et al.*, 2013) but are not often performed in SILAC studies.

Proteomic changes caused by oxidative/hypochlorite stress

Significant changes, in the proteome, were observed when *Hfx. volcanii* cells were treated with sublethal doses of NaOCl (2.5 mM for 20 min) designed to detect the first protein responders of hypochlorite stress. A total of 565 proteins was found to be of differential abundance due to the NaOCl treatment at a *p*-value of 0.05 or less (Supporting Information Table S6 and Fig. 3B). Of these differential proteins, 176 were found to be altered at least 1.5-fold: with 119 proteins up (Supporting Information Table S7) and 57 proteins down (Supporting Information Table S8) in abundance. Nearly half (85 proteins) of the 176 proteins had no predicted function by arCOG analysis (Fig. 4); however, some general trends in the differential proteome could be discerned by comparative genomics and protein homology modelling as outlined below.

ROS detoxification and sulfur mobilization. ROS detoxification and sulfur mobilization systems can promote redox balance and facilitate repair of sulfur-containing biomolecules, such as Fe—S clusters. Here, cysteine synthase (HVO_1439), cysteine desulfurase (HVO_A0635) and glutaredoxin/thioredoxin (Grx/Trx) (HVO_1081 and HVO_0337) homologs were found increased in abundance during hypochlorite stress. The sulfhydryl groups of cysteine and Grx/Trx may be used to facilitate the reduction of disulfide bonds (Fig. 2D) and to mobilize sulfur (e.g., via persulfide groups) for repair of sulfur-containing biomolecules during the hypochlorite stress. Surprisingly, peroxiredoxin (Prx), catalase-peroxidase (KatG), methionine sulfoxide reductase (MsrA/B), superoxide dismutase (SOD1/2) and other ROS detoxification systems, while detected, were not of differential abundance suggesting these enzymes were at sufficient levels during the early stages of hypochlorite stress. In *Hbs. salinarum, prx*, *sod1*, *msrA/B* and *katG* transcripts are detected at increased abundance during severe oxidative stress (Kaur *et al.*, 2010), while cysteine biosynthesis and *grx/trx* transcripts are found at elevated levels during both mild and severe ROS challenge (Whitehead *et al.*, 2006; Boubriak *et al.*, 2008; Kaur *et al.*, 2010). Thus, an increase in levels of the sulfhydryl containing cysteine and Grx/Trx proteins appears to be a common defense mechanism for ROS challenge in haloarchaea, while an increased abundance of ROS detoxification systems may be reserved for severe oxidative stress.

NAD$^+$/kynurenine metabolism. De novo biosynthesis of NAD$^+$ through kynurenine is redox sensitive and produces metabolic intermediates with the redox capacity to be protective and alter signal transduction (Crowley *et al.*, 2000; Massudi *et al.*, 2012; Gonzalez Esquivel *et al.*, 2017). Here, we found homologs of NAD$^+$ biosynthesis and kynurenine metabolism to be impacted at the protein level during hypochlorite stress including an increased abundance of nicotinamide-nucleotide adenylyltransferase (NadM, HVO_0782) and kynurenine formamidase (HVO_A0415) as well as a decreased abundance of nicotinate-nucleotide pyrophosphorylase [carboxylating] (NadC, HVO_2579) homologs. These results suggest ROS challenge may alter kynurenine/NAD$^+$ metabolism in *Hfx. volcanii*.

Ribosome biogenesis and translation. Proteins associated with ribosome biogenesis and translation were generally up during hypochlorite stress. Translation initiation factor IF-6 (HVO_0117), ribonuclease P (HVO_2556), an rRNA methylase (HVO_1669), a RimK-type ribosomal modification protein (HVO_0483) and 50S ribosomal proteins L44e (HVO_0701) and L13 (HVO_2778) were found highly up, while 10 other proteins of translation were found moderately up in abundance during the stress. Similarly, genes associated with translation are increased at the transcript level in *Hbs. salinarum* upon exposure to UV-C (McCready *et al*., 2005), UV-B (Boubriak *et al*., 2008), transition metals (Kaur *et al*., 2006), H_2O_2 and low doses of the superoxide (O_2^-) generating paraquat (Kaur *et al*., 2006; Kaur *et al*., 2010). Whether these ROS-stimulated changes cause an increase in translation that is used for protein repair or alter translation to stall/protect the ribosomal machinery during oxidative stress remains to be determined. In eukaryotes, ROS-mediated stress results in a general decrease in translation, increase in tRNA halves that can inhibit translation and preferential translation of mRNAs involved in the stress response (Holcik and Sonenberg, 2005; Thompson *et al*., 2008; Bakowska-Zywicka *et al*., 2016; Huang and Hopper, 2016).

Transcription and signal transduction. Transcription factor (TF) homologs dominated the proteins that were assigned general function and altered at least 1.5-fold in abundance during hypochlorite stress. Of the 176 proteins altered at least 1.5-fold, over 15% (27 proteins) were predicted TFs with most found increased in abundance (21 TFs up vs. 6 TFs down) during the NaOCl treatment. Many of these TFs had conserved Cys/His residues that could theoretically sense redox status including homologs related by Phyre2-modelling to bacterial TFs that mediate survival against oxidative stress [e.g., HypR (HVO_0855), DosR (HVO_A0563) and IscR (HVO_A0588)] (Crack *et al*., 2012; Chim *et al*., 2014; Hillion and Antelmann, 2015). Proteins associated with signal transduction were also found at elevated levels during hypochlorite stress including a soluble methyl-accepting chemotaxis (MCP) sensory transducer homolog (HVO_2220) and a CheY-like response regulator (HVO_2012) which may function in a coordinated manner. Likewise, up in abundance was a DUF336 family member (HVO_A0272) related to bacterial HbpS, a heam-degrading redox sensor that regulates catalase and peroxidase expression through interaction with a two-component signal transduction system (Ortiz de Orue Lucana *et al*., 2009). HVO_0215 was also found highly up in abundance during stress, and while the function of this TM protein remains to be determined, its predicted location in the cell membrane, conserved Fe-S cluster, haem-binding motif and lack of Fe-only hydrogenase active site residues suggests it may sense ROS challenge.

Metal homeostasis. High intracellular Mn/Fe ratios (Daly *et al*., 2004; Fredrickson *et al*., 2008; Kish *et al*., 2009) and metabolite complexes of Mn^{2+} (e.g., Mn-orthophosphate) (Daly *et al*., 2010; Culotta and Daly, 2013) are correlated with combating ROS stress and protecting proteins from oxidative damage. Proteomic responses of *Hfx. volcanii* that may promote a high Mn/Fe ratio were identified during hypochlorite stress. In particular, homologs (HVO_2397 and HVO_2398) of Mn^{2+}/Zn^{2+} transporters (Desrosiers *et al*., 2007; Wichgers Schreur *et al*., 2011) and the ferritin-like DpsA (HVO_0536) were found up in abundance during hypochlorite stress. In *Hbs. salinarum*, DpsA binds Fe^{2+} (Zeth *et al*., 2004) and is upregulated at the transcript level by ROS challenge (Reindel *et al*., 2005; Kaur *et al*., 2010) suggesting *Hfx. volcanii* DpsA could sequester the free pools of Fe^{2+} that exacerbate ROS challenge. Homologs of siderophore biosynthesis (HVO_B0041 to _B0044) and heavy metal (Cu^{2+}) transport (HVO_1751 of arCOG01576) were found significantly down in abundance, suggesting the uptake of Fe^{2+} and Cu^{2+} are reduced during hypochlorite stress. Down in abundance was also the DtxR-type HTH domain (IPR022687) protein HVO_0538 of arCOG02101 that includes *Hbs. salinarum* Idr2 (VNG0835G), a direct activator of putative siderophore biosynthesis gene expression and member of a transcriptional network that maintains Fe homeostasis (Schmid *et al*., 2011; Martinez-Pastor *et al*., 2017). Overall, the observed changes in the *Hfx. volcanii* proteome suggest hypochlorite stress signaled an increase in intracellular Mn/Fe ratios to protect the cells from ROS damage by altering the abundance of proteins associated with heavy metal uptake and Fe^{2+}-binding.

Small proteins of unknown function. Hypochlorite stress impacted the abundance of numerous small proteins. The levels of six small CPxCG-related ‘Zn finger’ proteins were altered by the stress including increased abundance of HVO_1359 (68 aa), HVO_2057A (59 aa), HVO_0720 (100 aa), HVO_2982 (67 aa) and HVO_0758 (56 aa) and decreased abundance of HVO_1352 (62 aa). These Zn finger proteins are predicted to coordinate divalent metal ion(s) through conserved His/Cys residues and form DNA, RNA and/or protein binding structures that regulate cell function. Of the Zn finger proteins, HVO_1352 and HVO_1359 were inversely correlated in abundance and encoded in genome synteny with HVO_1355, a small UPF0058 family protein (100 aa) that was up sixfold suggesting this region of the genome is highly related by ROS challenge. HVO_1355 is predicted to bind divalent metal based on comparison to its homolog *Hbs. salinarum*

Vng1086c (PDB: 2GF4). Other small proteins of unknown function altered by hypochlorite stress included HVO_1405 (147 aa), HVO_1563 (125 aa), HVO_2176 (66 aa), HVO_0805 (82 aa) and HVO_1516 (108 aa) that were increased in abundance and HVO_1512 (95 aa), HVO_1753 (65 aa), HVO_A0417 (102 aa), HVO_2897 (107 aa) and HVO_1188 (105 aa) that were decreased in abundance. By comparison, small CPxCG-related Zn finger proteins are increased at the transcript level by UV-mediated ROS challenge in *Hbs. salinarum* (McCready *et al*., 2005; Boubriak *et al*., 2008).

Lipid metabolism. Hypochlorite stress was found to increase the abundance of proteins associated with lipid metabolism by over 1.5-fold including homologs of *sn*-glycerol-1-phosphate dehydrogenase (HVO_0822, GldA), bifunctional short chain isoprenyl diphosphate synthase (HVO_2725, IsdA), farnesyl-diphosphate farnesyltransferase (HVO_1139, FdtF), glycerophosphodiester phosphodiesterase (HVO_B0291, GlpQ2), phosphatidylserine decarboxylase (HVO_0146, Psd) and a lipase/esterase homolog (HVO_0137). Of these, GldA forms the *sn*-glycerol-1-phosphate backbone of archaeal lipids (Caforio and Driessen, 2017) and is found increased at the transcript level by oxidative stress in *Hbs. salinarum* (Whitehead *et al*., 2006; Kaur *et al*., 2010). The increased abundance of proteins/transcripts associated with lipid metabolism may serve to replenish and/or modify the cell membrane and protect the haloarchaea from ROS damage.

DNA repair/recombination. DNA repair/recombination proteins were found increased in abundance during hypochlorite stress. Included in this group were the ATP-dependent helicase Hel308b (HVO_0971), Ski2-helical domain protein (HVO_0289), single-stranded-DNA-specific exonuclease RecJ1 (HVO_0073) and UvrC related protein (HVO_1745). Modest increases in abundance of the DNA repair/recombination associated DHH/RecJ family phosphoesterase RecJ3 (HVO_1018) and ssDNA binding replication protein A (RPA) (i.e., Rpa3 HVO_0292) of arCOG01510 were also observed. RPAs are widely associated with oxidative stress. In *Hbs. salinarum*, the RPAs are found overexpressed in extreme radiation-resistant mutants (DeVeaux *et al*., 2007) and increased in transcript level after ROS challenge (McCready *et al*., 2005; Whitehead *et al*., 2006; Boubriak *et al*., 2008; Kaur *et al*., 2010). Archaeal RPAs are thought to act as a platform for loading Hel308 helicases onto aberrant ssDNA at blocked replication forks (Woodman *et al*., 2011). Thus, the enhanced levels of Hel308b and RPA observed, here, during hypochlorite stress may serve to coordinate DNA repair. Note the *Hfx. volcanii* UvrC- and Ski2-like proteins found increased in abundance are missing their respective nuclease domains. While the UvrC-like HVO_1745 has the two helix-hairpin-helix (HhH) motif used for nonspecific DNA binding (Aravind *et al*., 1999), it is missing the RNase H domain and associated catalytic triad of UvrC (Karakas *et al*., 2007). Similarly, HVO_0289 is related to the C-terminal helical domain of Ski2 but lacks the central RecA1/2 domains needed for the helicase activity of Ski2 in eukaryotic exosome function (Halbach *et al*., 2012). The *Hfx. volcanii* Hel308 does have a RecA-like domain topology typical of Ski2 helicases (Woodman *et al*., 2011). Thus, the Hel308b, RPA and Ski2-like proteins may be coordinately increased in abundance during hypochlorite stress to repair DNA.

Archaeal RecJ proteins are generally associated with DNA repair, recombination and replication (Makarova *et al*., 2012; Oyama *et al*., 2016). Both *Hfx. volcanii* RecJ proteins found increased in abundance by hypochlorite stress had conserved nuclease active site residues, but were of distinct arCOG groups. HVO_0073 of arCOG00427 is a GINS-associated nuclease (GAN) homolog of the CMG (Cdc45/RecJ, MCM, GINS) complex of DNA replication and repair (Li *et al*., 2011; Oyama *et al*., 2016; Yi *et al*., 2017). By contrast, HVO_1018 is of arCOG00429 which includes: HAN (TK0155), a nuclease that binds Hef (helicase-associated endonuclease for fork-structured DNA)(Ishino *et al*., 2014) and VNG0779C, which is increased at the transcript level by UV radiation (McCready *et al*., 2005; Boubriak *et al*., 2008). While *Hfx. volcanii*, Hef (HVO_3010) is involved in stalled replication fork repair (Lestini *et al*., 2010; Lestini *et al*., 2013) and was detected in this study, the abundance of Hef was found unaltered by the hypochlorite stress.

UspA domain proteins. Of the 40 *Hfx. volcanii* proteins with UspA universal stress domains (IPR006016), four were found increased in abundance during hypochlorite stress: HVO_0428 (149 aa), HVO_0612 (143 aa), HVO_2156 (301 aa) and HVO_2500 (Cat2, 748 aa). Cat2 had an added N-terminal cationic amino acid/polyamine transporter 1 (IPR002293) domain which along with UspAs are associated with oxidative stress. UspAs are important for oxidative stress resistance in bacteria (Nachin *et al*., 2005; Liu *et al*., 2007) and for modulating ROS generation in plants (Gutierrez-Beltran *et al*., 2017). Likewise, overexpression of cationic amino acid transporters can alleviate oxidative stress in mammals (Konstantinidis *et al*., 2014; Rajapakse *et al*., 2014). In the halophilic methanogen *Methanohalophilus portucalensis*, the MJ0557-like UspA is increased at the transcript level by hypo-salt stress (Shih and Lai, 2010), UspAs are increased in protein abundance by low temperature growth in Antarctic haloarchaea (Williams *et al*., 2017) and the UspA-like KdpQ of *Hbs. salinarum* is implicated in K^+ homeostasis based on genome synteny (Strahl and Greie, 2008). Interestingly, little if any increase in abundance of UspA is noted at the transcript or protein level for *Hbs. salinarum* during recovery from ROS challenges that include gamma irradiation (Whitehead *et al*., 2006), H_2O_2/paraquat (Kaur *et al*., 2010), heavy metal (Kaur *et al*., 2006) and UV radiation (McCready *et al*., 2005; Boubriak *et al*., 2008). Thus, archaeal UspAs may be regulated by factors other than transcript level or are needed during specific stress conditions (e.g., hypochlorite, low temperature and hypo-saline).

Ion pumps/channels. By contrast to the cationic amino acid transporter Cat2, which was enhanced during hypochlorite stress, a decrease in abundance was observed for two ion channels: the small conductance mechanosensitive ion channel homolog MscS (HVO_1165) and the ion channel pore/TrkA domain protein PchA1 (HVO_1137). Ion channels are associated with dissipating membrane potential and altering the redox state of biomolecules (e.g., glutathione) (Lee *et al*., 2016).

Proteases and chaperones. Components of post-translational modification and protein quality control (chaperones/proteases) were found impacted by hypochlorite stress. HVO_0102, a homolog of the stress responsive Zn^{2+} metalloprotease HtpX that contributes to protein quality control in bacteria (Shimohata *et al*., 2002; Sakoh *et al*., 2005; Akiyama, 2009) was found increased in abundance along with various putative chaperones: the proteasome assembly chaperone PAC2 (HVO_0697), a metal insertion GTPase (UreG, HVO_0150) and various AAA ATPases [i.e., PAN2 (HVO_1957), Cdc48a (HVO_2380), Cdc48c (HVO_1327) and MoxR-like protein (HVO_1941)]. A von Willebrand factor (vWF) A domain protein (HVO_1256) that was a predicted structural homolog of the 26S proteasome ubiquitin receptor (Rpn10, PDB: 2X5N) was also increased in abundance. Of these, the vWF-like HVO_1256 and MoxR-like HVO_1941 may function together as a chaperone-like system based on analogy to RavA-ViaA (Wong *et al*., 2017). Overall, we found the levels of HtpX and molecular chaperones to be elevated, while the abundance of 20S proteasomes and Lon-type proteases to be unaffected during the early stages of hypochlorite stress.

Post-translational modification systems. The ubiquitin-like sampylation and N^{ε}-lysine acetylation pathways of protein modification were impacted by NaOCl treatment. In particular, the level of the ubiquitin-like SAMP1 (HVO_2619) was found to be enhanced during hypochlorite stress, in-line with our previous finding that samp1ylation is stimulated by the mild oxidant DMSO (Dantuluri *et al*., 2016). To support a role of SAMP1 in the hypochlorite stress response, we examined a Δ*samp1* mutant and found it to be hypersensitive to hypochlorite stress when compared to its parent (H26) (Fig. 5). Other known components of sampylation (SAMP2/3, MsrA, E1 UbaA and JAMM1/2)(Humbard *et al*., 2010; Miranda *et al*., 2011; Miranda *et al*., 2014; Fu *et al*., 2016; Cao *et al*., 2017; Fu *et al*., 2017) were detected, but not impacted in protein abundance by the stress. Instead, the abundance of putative structural homologs of eukaryotic ubiquitin-binding proteins were found to be increased by the hypochlorite stress including the SWIM Zn^{2+} finger domain protein HVO_A0396 [related to the MEX E3 ubiquitin ligase (Nishito *et al*., 2006)] and HVO_1514 [related to the JAMM1 desampylase (Cao *et al*., 2017) but unable to coordinate the catalytic Zn^{2+} ion] based on homology modelling. Regarding acetylation, the histone acetyltransferase (HAT) homologs Pat1/2 were found inversely correlated in abundance during stress: Pat1 (HVO_1756) was found down 3.1-fold, while Pat2 (HVO_1821) was up 1.8-fold in abundance. Pat1/2 are

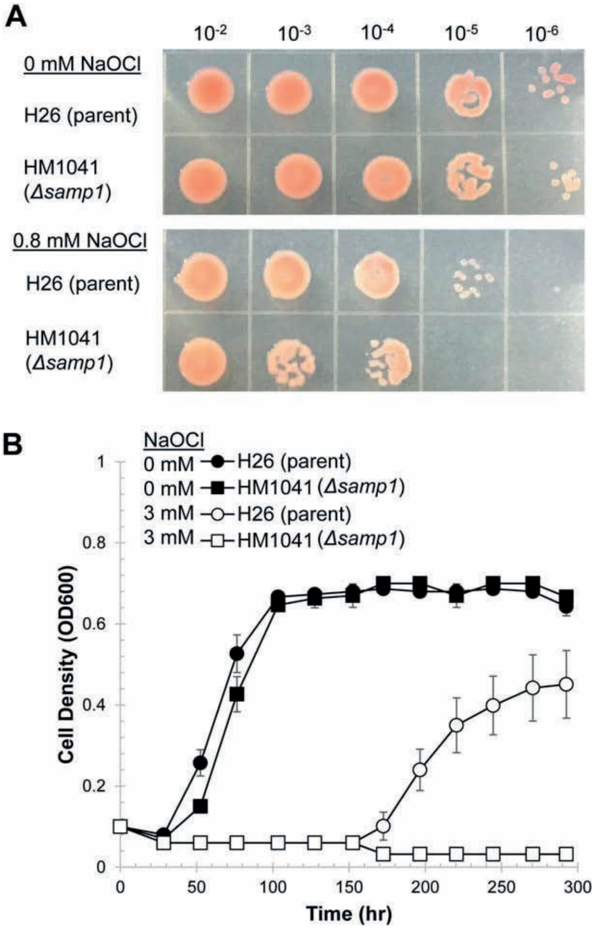

Fig. 5. Hypersensitivity of an *Hfx. volcanii* small archaeal ubiquitin-like modifier protein mutant (Δ*samp1*) to oxidative stress as predicted by SILAC and observed by treatment with NaOCl. H26 (parent) and HM1041 (Δsamp1) strains were spot plated by serial dilution (panel A) or grown in liquid culture (panel B) on glycerol minimal medium (GMM) with 0, 0.8 or 3 mM NaOCl as indicated. Error bars indicate standard deviation of $n = 9$ culture replicates with the experiment found reproducible ($n = 4$). See methods for details. [Colour figure can be viewed at wileyonlinelibrary.com]

proposed to mediate the N$^{\varepsilon}$-lysine acetylation of histones (Altman-Price and Mevarech, 2009). In eukaryotes, ubiquitination and acetylation of histones regulates chromatin structure (Caron *et al.*, 2005).

Conclusions

Here, we generated a SILAC-ready strain of *Hfx. volcanii* and studied quantitative differences in its proteome due to hypochlorite stress conditions. We generated lysine and arginine single and double auxotrophs of this archaeon which allowed for full isotopic incorporation and sensitive quantitative coverage of the proteome after trypsin digestion. In *Hfx. volcanii, lysA* and *argH* are now found essential in lysine and arginine biosynthesis, respectively. We identified 2565 proteins, covering 64% of the theoretical proteome (with a *q*-value of at least 0.01). While arginine to proline conversion is detected in the *Hfx. volcanii* LM08 strain at a rate of 34%, quantitative problems can be avoided by use of only one form of heavy arginine and may be overcome by deletion of *rocF* (HVO_1575) predicted to encode arginase (EC:3.5.3.1). We find the SILAC studies of *Hfx. volcanii* require only small amounts of cell material for whole-cell proteome studies, thus, minimizing costs. The SILAC method captured over half of the proteome, while maintaining coverage of membrane proteins, using 2 mg total protein (250 μg per replicate per experimental state). This method allows for conservative use of reagents, due to the small amount of protein needed and ability to reach 100% of theoretical labelling efficiency. The development of this strain now allows for multiplexed quantitative proteomic analysis with accurate relative abundance values in archaea. Our case study of hypochlorite stress provides guidance for future studies to uncover mechanisms used by haloarchaea to overcome ROS challenge.

Experimental procedures

Materials

Biochemicals were from Sigma Aldrich (St. Louis, MO, USA). Other inorganic and organic analytical grade chemicals were from Fisher-Scientific (Atlanta, GA, USA). Desalted oligonucleotide primers were from Integrated DNA Technologies (Coralville, IA, USA). Polymerases, ligase and restriction endonucleases were from New England Biolabs (Ipswich, MA, USA). Amino acid isotopes were from Cambridge Isotope Laboratories, Inc. (Tewksbury, MA, USA). Agarose for DNA analysis was purchased from Bio-Rad laboratories (Hercules, CA, USA).

Strains and media

Strains used in this study are listed in Table 2. *E. coli* strains Top10 and GM2163 were used for routine cloning and preparation of plasmid DNA for transformation into *Hfx. volcanii*, respectively (Dyall-Smith, 2009). *E. coli* strains were grown at 37°C in Luria-Bertani (LB) medium supplemented with ampicillin (0.1 mg·ml^{-1}). *Hfx. volcanii* strains were grown at 42°C at 200 r.p.m. rotary shaking in ATCC974 (complex) medium or GMM, the latter medium with ammonium chloride as the nitrogen source (Dyall-Smith, 2009). Media was supplemented with ampicillin (0.1 mg·ml^{-1}), novobiocin (0.1 μg·ml^{-1}), L-lysine or L-arginine as needed. L-Lysine and L-arginine concentrations were 0.3 mM unless specified otherwise. Culture plates were supplemented with 1.5% (w/v) agar for LB medium and 2.0% (w/v) agar for GMM and ATCC974 medium. Growth was measured by the optical density at 600 nm (OD_{600}) (where 1 OD_{600} unit equals approximately 10^9 CFU·ml^{-1}).

Generation of mutant strains

Plasmids and primers used in this study are listed in Table 2. Plasmids were constructed using one step sequence and ligation independent cloning (SLIC) (Jeong *et al.*, 2012). Gene deletions were created by the strategy shown previously by Allers and Ngo (2003). Gene homologs of *lysA* (HVO_1098; diaminopimelate decarboxylase EC 4.1.1.20) and *argH* (HVO_0048; argininosuccinate lyase EC 4.3.2.1) were targeted for markerless deletion on the *Hfx. volcanii* H26 genome. Colonies were screened for auxotrophy by growth on GMM plates with and without supplementation with L-arginine and/or L-lysine. The mutant strains were further analyzed by polymerase chain reaction (PCR) using genomic DNA as a template and primers that annealed outside of the plasmids used for homologous recombination. Mutants were further analyzed by Southern blotting in which genomic DNA was hybridized to digoxigenin-11-dUTP (Sigma Aldrich, St. Louis, MO, USA) labelled probes (Southern, 1975). The DNA hybrids were detected on the blots using alkaline phosphatase-conjugated antibody to digoxigenin and CDP-*Star* (Invitrogen, Thermo Fisher Scientific Waltham, MA, USA). The intensity of the DNA hybrid bands was visualized by X-ray film (Hyperfilm; Amersham Biosciences).

Growth assays for minimal amino acid

Hfx. volcanii Δ*lysA* and Δ*argH* mutants were tested for the minimum concentration of L-lysine and L-arginine required for optimal growth, respectively. Cells were grown in complex medium (ATCC974) to log phase (OD_{600} of 0.8). Cells were harvested by centrifugation (4000 × *g*), washed three times in GMM, resuspended in 5 ml GMM and subcultured to an OD_{600} of 0.01 in 25 ml of GMM supplemented with and without L-lysine or L-arginine (0 to 0.5 mM). Cultures were incubated with rotary shaking (200 r.p.m.) at 42°C in 125 ml Erlenmeyer flasks. Samples (0.1 to 1 ml) of culture were removed from 0 to 61 h for monitoring growth by OD_{600}.

Table 2. Strains, plasmids and oligonucleotide primers used in this study.[a]

Strain, plasmid or primer	Description	Source or reference
E. coli strains		
TOP10	F$^-$ *recA1 endA1 hsdR17*(r_K^- m_K^+) *supE44 thi-1gyrA relA1*	Invitrogen
GM2163	F$^-$ *ara-14 leuB6 fhuA31 lacY1 tsx78 glnV44 galK2 galT22 mcrA dcm-6 hisG4 rfbD1 rpsL136 dam13*::Tn*9 xylA5 mtl-1 thi-1 mcrB1 hsdR2*	New England Biolabs
H. volcanii strains		
DS70	wild-type isolate DS2 cured of plasmid pHV2	(Wendoloski *et al*., 2001)
H26	DS70 Δ*pyrE2*	(Allers *et al*., 2004)
LM06	H26 Δ*lysA (*hvo_1098)	This study
LM07	*H26* Δ*argH* (hvo_0048)	This study
LM08	H26 Δ*lysA* Δ*argH*	This study
HM1041	H26 Δ*samp1* (hvo_2619)	(Miranda *et al*., 2011)
Plasmids		
pTA131	Ap^r; pBluescript II containing P$_{fdx}$-pyrE2	(Allers *et al*., 2004)
pJAM2912	Ap^r; pTA131 based plasmid containing pre-deletion sequence for *lysA*	This study
pJAM2914	Ap^r; pTA131 based plasmid for Δ*lysA*	This study
pJAM2916	Ap^r; pTA131 based plasmid containing pre-deletion sequence for *argH*	This study
pJAM2917	Ap^r; pTA131 based plasmid for Δ*argH*	This study
pJAM202c	Ap^r Nv^r; Hfx. volcanii-E. coli shuttle P2$_{rrn}$ expression vector, empty vector	(Zhou *et al*., 2008)
pJAM2918	LysA complement	This study
pJAM2919	ArgH complement	This study
Primers		
LysA 500 up SLIC	5′ aggaattcgatatcaCCGCTATCACGACGTGCTCC 3′[a]	This study
LysA 500 dwn SLIC	5′ cggtatcgataagctTCCGGGAACACCGACGCGT 3′	This study
LysA inverse up	5′ TCACTCGCGCAGCGCCTCCTCC 3′	This study
LysA inverse dwn	5′ CCAAGCACCCACACAGAATCATGAGCGTACTCAA 5′	This study
LysA 700 up	5′ AGAAGACCGGCTCCGACGTGACCT 3′	This study
LysA 700 dwn	5′ ACTGCGTCTCGCCCTCGACG 3′	This study
LysAcompSLICfwd	5′ ctttaagaaggagatatacaATGAGCGGCGGCGGGC 3′	This study
LysAcompSLICrev	5′ tatgctagttattgctcataTCAGTTGGGGATGTGCTCGG3′	This study
ArgH 500 up SLIC	5′ aggaattcgatatcaAACTCATCTCGTTCCTCAA 3′	This study
ArgH 500 dwn SLIC	5′ cggtatcgataagctAGTCCAACGTGCAATTTA 3′	This study
ArgH inverse up	5′ CTTACTCGTCGCTACCGC 3′	This study
ArgH inverse dwn	5′ GTCCGAACGCGAGACGCC 5′	This study
ArgH 700 up	5′ TGGTCCATCGACACGAACCTCTG 3′	This study
ArgH 700 dwn	5′ AAGCGCGTGATGTAGATGCTCCTGC 3′	This study
ArgHcompSLICfwd	5′ ctttaagaaggagatataca ATGGCAGGCGAGGACGGCGACT 3′	This study
ArgHcompSLICrev	5′ tatgctagttattgctcataTCAGACATAGCTCGAAACCTCCTCGTCGAG 3′	This study

a. Sequence and ligase independent cloning (SLIC) overhangs to the plasmid vector are in lowercase.

Assays of cell survival after exposure to sodium hypochlorite (NaOCl)

Hfx. volcanii H26 cells were grown to log phase (OD$_{600}$ of 0.7) in 25 ml of GMM in 125 ml Erlenmeyer flasks in a rotary shaker (200 r.p.m.) at 42°C. To monitor survival after exposure to NaOCl, cells were treated with 0, 1.25, 2.5, 4 and 7.5 mM NaOCl (10 μl in dH$_2$O; diluted from Sigma Aldrich product 425044) at room temperature (RT) with 10 s of rotary shaking every 5 min for 20 min. Treated-cells were serially diluted in ATCC974 liquid and plated at 10^{-6} to 10^{-7} on ATCC974 plates. The colony forming units (CFU) per ml were determined to assess cell survival. To test recovery after long-term exposure of NaOCl, cells were grown to log phase as described above. The log phase cells were treated with 0, 2, 5, 8 and 11 mM NaOCl. Growth was monitored by OD$_{600}$ for 15 h after treatment, and cells were plated for survival on ATCC974 plates. Experiments were performed in biological triplicate. To compare survival of *Hfx. volcanii* HM1041 (Δ*samp1*) to its parent H26, the cells were streaked onto GMM agar from −80°C glycerol stocks and grown for 5 days in a closed plastic zippered bag at 42°C. Isolated colonies were inoculated into 3 ml GMM in a capped 13 × 100 mm culture tube and incubated at 42°C with rotary shaking (200 r.p.m.). At an OD$_{600}$ 0.9, the cultures were normalized to 1 OD unit · ml $^{-1}$ and serially diluted in GMM from 10^{-1} to 10^{-6}. Culture dilutions (20 μl) were spotted serially on GMM agar plates supplemented with 0.8 mM NaOCl and a mock control. Plates were placed in a closed plastic zippered bag in a 42°C incubator and allowed to grow for 5 days. As an added assay, H26 (parent) and HM1041 (Δ*samp1*) strains were streaked from −80°C glycerol stocks onto solid complex medium (ATCC974) and incubated as described above. Colonies were inoculated into 25 ml of ATCC974 medium in 125 ml Erlenmeyer flasks. Cells were grown to log phase (OD$_{600}$ of 0.6–0.8) at 42°C (200 r.p.m.). Cells were washed twice with GMM by centrifugation (8600 × *g*, 1 min at room temperature) and inoculated to a starting OD$_{600}$ of 0.1 unit in GMM (5 ml) supplemented with and without 3 mM NaOCl. Cells were incubated at 42°C (200 r.p.m.) in capped 13 × 100 mm culture tubes. Growth was monitored at OD_{600}.

Ellman's reagent assay for free sulfhydryl groups of NaOCl treated cells

Hfx. volcanii LM08 was grown to log phase (OD_{600} of 0.8) in 50 ml GMM supplemented with 0.3 mM L-lysine and 0.3 mM L-arginine in 125 ml Erlenmeyer flasks in a rotary shaker (200 r.p.m.) at 42°C. The cultures were immediately treated with 0 and 2.5 mM NaOCl in biological triplicate as described for survival assays. After the 20 min treatment, cells were pelleted at 4000 × *g* and resuspended in 1 ml reaction buffer (0.1 sodium phosphate pH 8.0 with 1 mM EDTA). Cells were lysed on ice by sonication (Sonic Dismembrator Model 500, Fisher Scientific) at 30% amplitude for 2 s on, 2 s off for 20 s total, three times over. Cell lysate was clarified by centrifugation at 13 000 × *g* and passed through a 0.2 μm surfactant-free cellulose acetate (SFCA) filter (Nalgene, ThermoFisher Scientific, USA). The filtrate was quantified for total protein by the bicinchoninic acid (BCA) assay (Pierce, USA) and assayed for thiol content by Ellman's reagent assay. In brief, the Ellman's reagent was generated by dissolving 4 mg of 5,5′-dithio-bis-(2-nitrobenzoic acid) (DTNB) (ThermoFisher Scientific) in 1 ml reaction buffer (0.1 M sodium phosphate, pH 8.0, containing 1 mM EDTA). Reactions (2.8 ml total volume) were mixtures of 50 μl Ellman's reagent, 0.25 ml protein (0.97 mg total) and 2.5 ml reaction buffer in borosilicate glass tubes (13 × 100 mm Fisher Scientific). The reactions were vortexed to mix and incubated at RT for 15 min. Sample (250 μl) was transferred in triplicate to a clear polystyrene flat bottom 96 well plate (Fisher Scientific) and absorbance was measured at 412 nm using a Biotek Synergy HTX Multi-Mode Reader. L-Cysteine hydrochloride monohydrate (Fisher BioReagents, Fisher Scientific) was used as a standard to quantify the sulfhydryl groups.

Isotopic incorporation

Hfx. volcanii LM08 was streaked with a toothpick from 20% v/v glycerol stocks stored at −80°C onto a plate of GMM supplemented with 0.5 mM lysine and 0.5 mM arginine and grown at 42°C for 5 days. Isolated colonies were transferred to 25 ml GMM supplemented with either heavy or light amino acids separately (0.3 mM each) and allowed to grow for 24 h (about 6.5 doublings) (in a 125 ml Erlenmeyer flask at 42°C in a rotary shaker at 200 r.p.m.). Cultures were subcultured into 25 ml GMM to a starting OD_{600} of 0.01 and similarly grown in the same heavy or light medium for 24 h, twice sequentially for a total of three subcultures after 24 h each. The heavy amino acids were L-lysine + 8 (L-lysine: 2HCl, $^{13}C_6$, 99%; $^{15}N_2$, 99%; Item No. CNLM-291-H-PK) and L-arginine + 6 (L-arginine: HCl, $^{13}C_6$, 99%; Item No. CLM-2265-H-PK) (Cambridge Isotope Laboratories). The light amino acids were L-lysine and L-arginine purchased from Sigma Aldrich (Item No. L8662 and A8094, respectively). The final cultures were harvested at log phase (OD_{600} 0.6) by centrifugation at 4000 × *g*. Proteins were extracted with TRIzol (ThermoFisher Scientific) as described previously (Kirkland *et al.*, 2006). A preliminary study was done to determine the incorporation rate of heavy lysine (+8) and heavy arginine (+6) into the proteome. These preliminary untreated samples were analyzed by LC-MS/MS to monitor isotope incorporation, as described below, with the following exceptions: (1) sulfhydryl groups of the proteins were alkylated by reacting with 50 mM iodoacetamide in the dark at room temperature for 45 min, (2) tryptic peptides were separated by a 60 min linear gradient with the Easy-nLC 1200 system, (3) strong cation exchange (SCX) was not used for separation of peptides and (4) peptide masses were detected by a Q Exactive Plus Hybrid Quadrupole-Orbitrap Mass Spectrometer.

Experimental design

Four biological replicates (*n* = 4) of the *Hfx. volcanii* LM08 cells were grown in 25 ml of GMM at 42°C in a rotary shaker (200 r.p.m.) to late log phase (OD_{600} 0.7–0.8). The cells were incubated for 20 min with 2.5 mM NaOCl (treatment groups) or dH_2O (control groups) as described for the survival assays. For two of the biological replicates, the control group cultures were labelled with (heavy) L-lysine (+8) and L-arginine (+6) and the treatment group was labelled with (light) L-lysine (+0) and L-arginine (+0), as described above. The other two replicates were grown with the labels switched: (heavy) L-lysine + 8 and L-arginine + 6 for the treatment group and (light) L-lysine + 0 and L-arginine + 0 for the control. This experimental designed allowed for comparison of the label swap as well as an assessment of the impact of oxidative stress on the *Hfx. volcanii* proteome.

Preparation of protein samples for analysis by mass spectrometry

Culture volumes were normalized in each centrifuge tube to equivalent total OD units per sample, and cells were harvested by centrifugation (4000 × *g*). All supernatant was carefully removed. The cell pellets were stored at −80°C. Cell pellets of control and treatment groups were mixed at a 1:1 ratio (*n* = 4 mixed samples), and the proteins were extracted with TRIzol, as described previously (Kirkland *et al.*, 2006). The protein pellets were stored at −20°C and processed as described previously (Mostafa *et al.*, 2016) with a few modifications. Pellets were dissolved in a solubilization buffer [7 M urea, 2 M thiourea and 4% (w/v) CHAPS] and quantified by EZQ assay kit (Weist *et al.*, 2008) according to manufacturer instructions (Invitrogen Inc., Eugene, OR, USA). Protein (500 μg per 100 μl buffer) was reduced by addition of 2.5 μl of 50 mM tris-(2-carboxyethyl phosphine (TCEP) and incubating the sample at 60°C for 60 min. After cooling the sample, the protein was treated with 5 μl of 200 mM methyl methanethiosulfonate (MMTS) for 30 min in the dark and digested with 5 μg modified trypsin (Promega, Madison, WI, USA) at 37°C for 16 h. Peptides were lyophilized and solubilized in 3% v/v acetonitrile in 0.1% v/v formic acid and desalted on a Macrospin C-18 reverse phase mini-column (The Nestgroup Inc., Southborough, MA, USA). Eluted peptides were lyophilized and fractionated by strong cation exchange chromatography (SCX) as described previously (Zhu *et al.*, 2010) with gradient as in (Mostafa *et al.*, 2016) at a flow rate of 200 μl/min. In brief, solvent A (25% v/v acetonitrile, 10 mM ammonium formate and 0.1% v/v formic acid, pH 2.8) was applied for 10 min and a linear gradient of 0%–20% solvent B (25% v/v acetonitrile and 500 mM ammonium formate, pH 6.8) was applied over 80 min before applying another 5 min gradient to 100% solvent B and holding for 10 min. Peptide elution was monitored by absorbance at 280 nm (A_{280}). SCX fractions (14 total) were pooled and lyophilized. In addition, replicate 1 had one postrun fraction and replicates 2–4 have 5 postrun fractions that were included in the LC-MS/MS analysis.

Reversed-phase liquid chromatography tandem mass spectrometry (LC-MS/MS) analysis

Fractions were resuspended in LC solvent A (0.1% v/v formic acid in 3% v/v acetonitrile) and analyzed one at a time on an Easy-nLC 1200 system coupled to a Q-Exactive Orbitrap Plus MS (Thermo Fisher Scientific, Bremen, Germany). Peptides were concentrated on an Acclaim Pepmap 100 pre-column (20 mm × 75 μm; 3 μm-C18) and separated on a PepMap RSLC analytical column (250 mm × 75 μm; 2 μm-C18) at a flow rate of 300 nl/min using solvent A (0.1% v/v formic acid) and B (0.1% v/v formic acid and 99.9% v/v acetonitrile) at a gradient of 2%–30% solvent B in 100 min, 30%–98% solvent B in 10 min before an isocratic flow of 98% solvent B for 10 min. The separated peptides were analyzed on a Q-Exactive Plus MS (Thermo Fisher Scientific, Bremen, Germany) in positive ion mode and top 10 data dependent scanning with high collision dissociation (HCD) as previously described (Mostafa *et al.*, 2016). Briefly, the spray voltage was 1800 V. The full MS resolution was 70 000 with a scan range of 350–1800 *m/z*, an AGC target of 3e6 and maximum IT of 250 ms. The MS/MS resolution was 17 500 with a scan range of 200–2000 *m/z*, an AGC target of 5e5 and maximum IT of 50 ms, the normalized collision energy of 27. The underfill ratio was 1%, intensity threshold was 2e5, charge exclusion was unassigned, 1, 7–8 and >8.

Data analysis and statistical rationale

Proteome Discoverer 2.1 (Thermo Scientific, Bremen, Germany) was used for protein identification and quantitation using the *Hfx. volcanii* DS2 database (downloaded from www.Uniprot.org April 2017) with 3996 entries and NTRANS_0004 (Ammar *et al.*, 2012). Proteome Discoverer was also used to generate the decoy database of the *Hfx. volcanii* proteome that was used to estimate the false discovery rate (FDR). Peptide and protein identification was set to an FDR adjusted *p*-value (or *q*-value) of 0.01 or less implying that 1% of significant tests would result in false positives. cRAP database was also searched for protein contaminants (none were detected at a *q*-value of 0.01 or less). Peptides were allowed two missed cleavages by trypsin and a static modification of methylthio on all cysteines. Dynamic modifications allowed were lysine +8, arginine +6, proline +5, methionine oxidation, N-terminal acetylation and diglycine remnant on lysines. Mass tolerance for precursor ions was 10 ppm. Mass tolerance for fragment ions was 0.02 Da. Peptide abundances were mean normalized and scaled by Proteome Discoverer. Peptides identified for each protein were used to find the statistical significance of protein abundance using Welch's *t*-test in R (version 3.3.3) to a *p*-value of < 0.05 (Cox *et al.*, 2014). Ambiguous peptides and peptides with no or nonunique quantitative information were excluded in the analysis. The 50 most abundant proteins and 50 least abundant proteins were identified using the highest and lowest exponentially modified protein abundance index (emPAI) values, respectively (Ishihama *et al.*, 2005). For the least abundant proteins, the proteins were identified in at least three replicates and the most abundant proteins were found in all four replicates. The effect of label swapping was tested using Welch's *t*-test at *p*-value < 0.01 using the peptide abundances from the control groups in the 50 most abundant proteins by emPAI value found in all four replicates. Proline conversion was calculated by taking the top three most abundant proteins by emPAI value and counting the number of heavy prolines (+5) out of total proline residues. Protein arCOG information (Makarova *et al.*, 2007) was found in www.uniprot.org (The UniProt Consortium, 2017). Transmembrane domains were determined by Expasy TMpred server (Hofmann and Stoffel, 1993). The mass spectrometry proteomics data have been deposited to the ProteomeXchange Consortium via the PRIDE (Vizcaino *et al.*, 2016) partner repository with the dataset identifier PXD006877 (Username: reviewer36568@ebi.ac.uk and Password: IqT96pAU).

Acknowledgements

The authors thank S. Shanker at the UF ICBR Genomics Core for Sanger DNA sequencing, staff at the UF ICBR Proteomics Core for assisting in Mass Spectrometry and Guido Pardi IV for writing programs to facilitate data analysis. Author contributions: LM, SH, JK, SC and JM-F designed the research and analyzed the data. LM and JM-F wrote the paper. LM, SH, JK and RF performed the research. All authors read and approve of the paper. Funds awarded to JM-F for this project were through the Bilateral NSF/BIO-BBSRC program (NSF 1642283), U.S. Department of Energy, Office of Basic Energy Sciences, Division of Chemical Sciences, Geosciences and Biosciences, Physical Biosciences Program (DOE DE-FG02-05ER15650) and the National Institutes of Health (NIH R01 GM57498). The authors do not have a conflict of interest to declare.

References

Akiyama, Y. (2009) Quality control of cytoplasmic membrane proteins in *Escherichia coli*. *J Biochem* **146:** 449–454.

Allers, T., and Ngo, H.P. (2003) Genetic analysis of homologous recombination in Archaea: *Haloferax volcanii* as a model organism. *Biochem Soc Trans* **31:** 706–710.

Allers, T., Ngo, H.P., Mevarech, M., and Lloyd, R.G. (2004) Development of additional selectable markers for the halophilic archaeon *Haloferax volcanii* based on the *leuB* and *trpA* genes. *Appl Environ Microbiol* **70:** 943–953.

Allers, T., Barak, S., Liddell, S., Wardell, K., and Mevarech, M. (2010) Improved strains and plasmid vectors for conditional overexpression of His-tagged proteins in *Haloferax volcanii*. *Appl Environ Microbiol* **76:** 1759–1769.

Altman-Price, N., and Mevarech, M. (2009) Genetic evidence for the importance of protein acetylation and protein deacetylation in the halophilic archaeon *Haloferax volcanii*. *J Bacteriol* **191:** 1610–1617.

Ammar, R., Torti, D., Tsui, K., Gebbia, M., Durbic, T., Bader, G.D., *et al*. (2012) Chromatin is an ancient innovation conserved between Archaea and Eukarya. *Elife* **1:** e00078.

Aravind, L., Walker, D.R., and Koonin, E.V. (1999) Conserved domains in DNA repair proteins and evolution of repair systems. *Nucleic Acids Res* **27:** 1223–1242.

Bakowska-Zywicka, K., Kasprzyk, M., and Twardowski, T. (2016) tRNA-derived short RNAs bind to *Saccharomyces cerevisiae* ribosomes in a stress-dependent manner and inhibit protein synthesis *in vitro*. *FEMS Yeast Res* **16:** pii: fow077.

Beck, M., Schmidt, A., Malmstroem, J., Claassen, M., Ori, A., Szymborska, A., *et al*. (2011) The quantitative proteome of a human cell line. *Mol Syst Biol* **7:** 549.

Bendall, S.C., Hughes, C., Stewart, M.H., Doble, B., Bhatia, M., and Lajoie, G.A. (2008) Prevention of amino acid conversion in SILAC experiments with embryonic stem cells. *Mol Cell Proteomics* **7:** 1587–1597.

Bicho, C.C., de Lima Alves, F., Chen, Z.A., Rappsilber, J., and Sawin, K.E. (2010) A genetic engineering solution to the “arginine conversion problem” in stable isotope labeling by amino acids in cell culture (SILAC). *Mol Cell Proteomics* **9:** 1567–1577.

Bidle, K.A., Kirkland, P.A., Nannen, J.L., and Maupin-Furlow, J.A. (2008) Proteomic analysis of *Haloferax volcanii* reveals salinity-mediated regulation of the stress response protein PspA. *Microbiology* **154:** 1436–1443.

Boubriak, I., Ng, W.L., DasSarma, P., DasSarma, S., Crowley, D.J., and McCready, S.J. (2008) Transcriptional responses to biologically relevant doses of UV-B radiation in the model archaeon, *Halobacterium* sp. NRC-1. *Saline Systems* **4:** 13.

Butter, F., Bucerius, F., Michel, M., Cicova, Z., Mann, M., and Janzen, C.J. (2013) Comparative proteomics of two life cycle stages of stable isotope-labeled *Trypanosoma brucei* reveals novel components of the parasite’s host adaptation machinery. *Mol Cell Proteomics* **12:** 172–179.

Cabiscol, E., Tamarit, J., and Ros, J. (2000) Oxidative stress in bacteria and protein damage by reactive oxygen species. *Int Microbiol* **3:** 3–8.

Caforio, A., and Driessen, A.J.M. (2017) Archaeal phospholipids: structural properties and biosynthesis. *Biochim Biophys Acta* **1862:** 1325–1339.

Cao, S., Engilberge, S., Girard, E., Gabel, F., Franzetti, B., and Maupin-Furlow, J.A. (2017) Structural insight into ubiquitin-like protein recognition and oligomeric states of JAMM/MPN+ proteases. *Structure* **25:** 823–833.e6.

Caron, C., Boyault, C., and Khochbin, S. (2005) Regulatory cross-talk between lysine acetylation and ubiquitination: role in the control of protein stability. *Bioessays* **27:** 408–415.

Cerletti, M., Paggi, R.A., Guevara, C.R., Poetsch, A., and De Castro, R.E. (2015) Global role of the membrane protease LonB in Archaea: potential protease targets revealed by quantitative proteome analysis of a *lonB* mutant in *Haloferax volcanii*. *J Proteomics* **121:** 1–14.

Chim, N., Johnson, P.M., and Goulding, C.W. (2014) Insights into redox sensing metalloproteins in *Mycobacterium tuberculosis*. *J Inorg Biochem* **133:** 118–126.

Cox, J., Hein, M.Y., Luber, C.A., Paron, I., Nagaraj, N., and Mann, M. (2014) Accurate proteome-wide label-free quantification by delayed normalization and maximal peptide ratio extraction, termed MaxLFQ. *Mol Cell Proteomics* **13:** 2513–2526.

Crack, J.C., Green, J., Hutchings, M.I., Thomson, A.J., and Le Brun, N.E. (2012) Bacterial iron-sulfur regulatory proteins as biological sensor-switches. *Antioxid Redox Signal* **17:** 1215–1231.

Crowley, C.L., Payne, C.M., Bernstein, H., Bernstein, C., and Roe, D. (2000) The NAD^+ precursors, nicotinic acid and nicotinamide protect cells against apoptosis induced by a multiple stress inducer, deoxycholate. *Cell Death Differ* **7:** 314–326.

Culotta, V.C., and Daly, M.J. (2013) Manganese complexes: diverse metabolic routes to oxidative stress resistance in prokaryotes and yeast. *Antioxid Redox Signal* **19:** 933–944.

Daly, M.J., Gaidamakova, E.K., Matrosova, V.Y., Vasilenko, A., Zhai, M., Venkateswaran, A., *et al*. (2004) Accumulation of Mn(II) in *Deinococcus radiodurans* facilitates gamma-radiation resistance. *Science* **306:** 1025–1028.

Daly, M.J., Gaidamakova, E.K., Matrosova, V.Y., Kiang, J.G., Fukumoto, R., Lee, D.Y., *et al*. (2010) Small-molecule antioxidant proteome-shields in *Deinococcus radiodurans*. *PLoS One* **5:** e12570.

Dantuluri, S., Wu, Y., Hepowit, N.L., Chen, H., Chen, S., and Maupin-Furlow, J.A. (2016) Proteome targets of ubiquitin-like samp1ylation are associated with sulfur metabolism and oxidative stress in *Haloferax volcanii*. *Proteomics* **16:** 1100–1110.

Dennis, W.H., Olivieri, V.P., and Krusé, C.W. (1979) The reaction of nucleotides with aqueous hypochlorous acid. *Water Res* **13:** 357–362.

Desrosiers, D.C., Sun, Y.C., Zaidi, A.A., Eggers, C.H., Cox, D.L., and Radolf, J.D. (2007) The general transition metal (Tro) and Zn^{2+} (Znu) transporters in *Treponema pallidum*: analysis of metal specificities and expression profiles. *Mol Microbiol* **65:** 137–152.

DeVeaux, L.C., Muller, J.A., Smith, J., Petrisko, J., Wells, D.P., and DasSarma, S. (2007) Extremely radiation-resistant mutants of a halophilic archaeon with increased single-stranded DNA-binding protein (RPA) gene expression. *Radiat Res* **168:** 507–514.

Dyall-Smith, M. (2009) *The halohandbook: protocols for halobacterial genetics* [WWW document]. URL http://www.haloarchaea.com/resources/halohandbook/Halohandbook_2009_v7.2mds.pdf.

Fredrickson, J.K., Li, S.M., Gaidamakova, E.K., Matrosova, V.Y., Zhai, M., Sulloway, H.M., *et al*. (2008) Protein oxidation: key to bacterial desiccation resistance? *ISME J* **2:** 393–403.

Fu, X., Liu, R., Sanchez, I., Silva-Sanchez, C., Hepowit, N.L., Cao, S., *et al*. (2016) Ubiquitin-like proteasome system represents a eukaryotic-like pathway for targeted proteolysis in archaea. *mBio* **7:** pii: e00379–e00316.

Fu, X., Adams, Z., Liu, R., Hepowit, N.L., Wu, Y., Bowmann, C.F., *et al*. (2017) Methionine sulfoxide reductase A (MsrA) and its function in ubiquitin-like protein modification in Archaea. *MBio* **8:** e01169–e01217.

Gonzalez Esquivel, D., Ramirez-Ortega, D., Pineda, B., Castro, N., Rios, C., and Perez de la Cruz, V. (2017) Kynurenine pathway metabolites and enzymes involved in redox reactions. *Neuropharmacology* **112:** 331–345.

Gutierrez-Beltran, E., Personat, J.M., de la Torre, F., and Del Pozo, O. (2017) A universal stress protein involved in oxidative stress is a phosphorylation target for protein kinase CIPK6. *Plant Physiol* **173:** 836–852.

Halbach, F., Rode, M., and Conti, E. (2012) The crystal structure of *S. cerevisiae* Ski2, a DExH helicase associated with the cytoplasmic functions of the exosome. *RNA* **18:** 124–134.

Hillion, M., and Antelmann, H. (2015) Thiol-based redox switches in prokaryotes. *Biol Chem* **396:** 415–444.

Hofmann, K., and Stoffel, W. (1993) TMbase – a database of membrane spanning proteins segments. *Biol Chem Hoppe-Seyler* **374:** 166.

Holcik, M., and Sonenberg, N. (2005) Translational control in stress and apoptosis. *Nat Rev Mol Cell Biol* **6:** 318–327.

Huang, H.Y., and Hopper, A.K. (2016) Multiple layers of stress-induced regulation in tRNA biology. *Life (Basel)* **6:** 16.

Humbard, M.A., Zhou, G., and Maupin-Furlow, J.A. (2009) The N-terminal penultimate residue of 20S proteasome alpha1 influences its N^{α} acetylation and protein levels as well as growth rate and stress responses of *Haloferax volcanii*. *J Bacteriol* **191:** 3794–3803.

Humbard, M.A., Miranda, H.V., Lim, J.M., Krause, D.J., Pritz, J.R., Zhou, G., *et al.* (2010) Ubiquitin-like small archaeal modifier proteins (SAMPs) in *Haloferax volcanii*. *Nature* **463:** 54–60.

Ishihama, Y., Oda, Y., Tabata, T., Sato, T., Nagasu, T., Rappsilber, J., and Mann, M. (2005) Exponentially modified protein abundance index (emPAI) for estimation of absolute protein amount in proteomics by the number of sequenced peptides per protein. *Mol Cell Proteomics* **4:** 1265–1272.

Ishino, S., Yamagami, T., Kitamura, M., Kodera, N., Mori, T., Sugiyama, S., *et al.* (2014) Multiple interactions of the intrinsically disordered region between the helicase and nuclease domains of the archaeal Hef protein. *J Biol Chem* **289:** 21627–21639.

Jeong, J.Y., Yim, H.S., Ryu, J.Y., Lee, H.S., Lee, J.H., Seen, D.S., and Kang, S.G. (2012) One-step sequence- and ligation-independent cloning as a rapid and versatile cloning method for functional genomics studies. *Appl Environ Microbiol* **78:** 5440–5443.

Jones, D.L., and Baxter, B.K. (2017) DNA repair and photoprotection: mechanisms of overcoming environmental ultraviolet radiation exposure in halophilic archaea. *Front Microbiol* **8:** 1882.

Karakas, E., Truglio, J.J., Croteau, D., Rhau, B., Wang, L., Van Houten, B., and Kisker, C. (2007) Structure of the C-terminal half of UvrC reveals an RNase H endonuclease domain with an Argonaute-like catalytic triad. *EMBO J* **26:** 613–622.

Kaur, A., Pan, M., Meislin, M., Facciotti, M.T., El-Gewely, R., and Baliga, N.S. (2006) A systems view of haloarchaeal strategies to withstand stress from transition metals. *Genome Res* **16:** 841–854.

Kaur, A., Van, P.T., Busch, C.R., Robinson, C.K., Pan, M., Pang, W.L., *et al.* (2010) Coordination of frontline defense mechanisms under severe oxidative stress. *Mol Syst Biol* **6:** 393.

Kirkland, P.A., Busby, J., Stevens, S., Jr, and Maupin-Furlow, J.A. (2006) Trizol-based method for sample preparation and isoelectric focusing of halophilic proteins. *Anal Biochem* **351:** 254–259.

Kirkland, P.A., Humbard, M.A., Daniels, C.J., and Maupin-Furlow, J.A. (2008) Shotgun proteomics of the haloarchaeon *Haloferax volcanii*. *J Proteome Res* **7:** 5033–5039.

Kish, A., Kirkali, G., Robinson, C., Rosenblatt, R., Jaruga, P., Dizdaroglu, M., and DiRuggiero, J. (2009) Salt shield: intracellular salts provide cellular protection against ionizing radiation in the halophilic archaeon, *Halobacterium salinarum* NRC-1. *Environ Microbiol* **11:** 1066–1078.

Konstantinidis, G., Head, G.A., Evans, R.G., Nguyen-Huu, T.P., Venardos, K., Croft, K.D., *et al.* (2014) Endothelial cationic amino acid transporter-1 overexpression can prevent oxidative stress and increases in arterial pressure in response to superoxide dismutase inhibition in mice. *Acta Physiol (Oxf)* **210:** 845–853.

Kort, J.C., Esser, D., Pham, T.K., Noirel, J., Wright, P.C., and Siebers, B. (2013) A cool tool for hot and sour Archaea: proteomics of *Sulfolobus solfataricus*. *Proteomics* **13:** 2831–2850.

Lee, C.P., Maksaev, G., Jensen, G.S., Murcha, M.W., Wilson, M.E., Fricker, M., *et al.* (2016) MSL1 is a mechanosensitive ion channel that dissipates mitochondrial membrane potential and maintains redox homeostasis in mitochondria during abiotic stress. *Plant J* **88:** 809–825.

Lestini, R., Duan, Z., and Allers, T. (2010) The archaeal Xpf/Mus81/FANCM homolog Hef and the Holliday junction resolvase Hjc define alternative pathways that are essential for cell viability in *Haloferax volcanii*. *DNA Repair (Amst)* **9:** 994–1002.

Lestini, R., Laptenok, S.P., Kühn, J., Hink, M.A., Schanne-Klein, M.C., Liebl, U., and Myllykallio, H. (2013) Intracellular dynamics of archaeal FANCM homologue Hef in response to halted DNA replication. *Nucleic Acids Res* **41:** 10358–10370.

Li, Z., Pan, M., Santangelo, T.J., Chemnitz, W., Yuan, W., Edwards, J.L., *et al.* (2011) A novel DNA nuclease is stimulated by association with the GINS complex. *Nucleic Acids Res* **39:** 6114–6123.

Liu, W.T., Karavolos, M.H., Bulmer, D.M., Allaoui, A., Hormaeche, R.D., Lee, J.J., and Khan, C.M. (2007) Role of the universal stress protein UspA of *Salmonella* in growth arrest, stress and virulence. *Microb Pathog* **42:** 2–10.

Makarova, K.S., Sorokin, A.V., Novichkov, P.S., Wolf, Y.I., and Koonin, E.V. (2007) Clusters of orthologous genes for 41 archaeal genomes and implications for evolutionary genomics of archaea. *Biol Direct* **2:** 33.

Makarova, K.S., Koonin, E.V., and Kelman, Z. (2012) The CMG (CDC45/RecJ, MCM, GINS) complex is a conserved component of the DNA replication system in all archaea and eukaryotes. *Biol Direct* **7:** 7.

Martinez-Pastor, M., Lancaster, W.A., Tonner, P.D., Adams, M.W.W., and Schmid, A.K. (2017) A transcription network of interlocking positive feedback loops maintains intracellular iron balance in archaea. *Nucleic Acids Res* **45:** 9990–10001.

Massudi, H., Grant, R., Guillemin, G.J., and Braidy, N. (2012) NAD^+ metabolism and oxidative stress: the golden nucleotide on a crown of thorns. *Redox Rep* **17:** 28–46.

McCready, S., Muller, J.A., Boubriak, I., Berquist, B.R., Ng, W.L., and DasSarma, S. (2005) UV irradiation induces homologous recombination genes in the model archaeon, *Halobacterium* sp. NRC-1. *Saline Systems* **1:** 3.

Megger, D.A., Pott, L.L., Ahrens, M., Padden, J., Bracht, T, Kuhlmann, K., *et al*. (2014) Comparison of label-free and label-based strategies for proteome analysis of hepatoma cell lines. *Biochim Biophys Acta* **1844:** 967–976.

Miranda, H.V., Nembhard, N., Su, D., Hepowit, N., Krause, D.J., Pritz, J.R., *et al*. (2011) E1- and ubiquitin-like proteins provide a direct link between protein conjugation and sulfur transfer in archaea. *Proc Natl Acad Sci USA* **108:** 4417–4422.

Miranda, H.V., Antelmann, H., Hepowit, N., Chavarria, N.E., Krause, D.J., Pritz, J.R., *et al*. (2014) Archaeal ubiquitin-like SAMP3 is isopeptide-linked to proteins via a UbaA-dependent mechanism. *Mol Cell Proteomics* **13:** 220–239.

Mostafa, I., Zhu, N., Yoo, M.J., Balmant, K.M., Misra, B.B., Dufresne, C., *et al*. (2016) New nodes and edges in the glucosinolate molecular network revealed by proteomics and metabolomics of Arabidopsis *myb28/29* and *cyp79B2/B3* glucosinolate mutants. *J Proteomics* **138:** 1–19.

Nachin, L., Nannmark, U., and Nystrom, T. (2005) Differential roles of the universal stress proteins of *Escherichia coli* in oxidative stress resistance, adhesion, and motility. *J Bacteriol* **187:** 6265–6272.

Nishito, Y., Hasegawa, M., Inohara, N., and Nunez, G. (2006) MEX is a testis-specific E3 ubiquitin ligase that promotes death receptor-induced apoptosis. *Biochem J* **396:** 411–417.

Ong, S.E., and Mann, M. (2006) A practical recipe for stable isotope labeling by amino acids in cell culture (SILAC). *Nat Protoc* **1:** 2650–2660.

Ong, S.E., Blagoev, B., Kratchmarova, I., Kristensen, D.B., Steen, H., Pandey, A., and Mann, M. (2002) Stable isotope labeling by amino acids in cell culture, SILAC, as a simple and accurate approach to expression proteomics. *Mol Cell Proteomics* **1:** 376–386.

Ong, S.E., Kratchmarova, I., and Mann, M. (2003) Properties of 13C-substituted arginine in stable isotope labeling by amino acids in cell culture (SILAC). *J Proteome Res* **2:** 173–181.

Ortiz-Bermudez, P., Srebotnik, E., and Hammel, K.E. (2003) Chlorination and cleavage of lignin structures by fungal chloroperoxidases. *Appl Environ Microbiol* **69:** 5015–5018.

Ortiz de Orue Lucana, D., Bogel, G., Zou, P., and Groves, M.R. (2009) The oligomeric assembly of the novel haem-degrading protein HbpS is essential for interaction with its cognate two-component sensor kinase. *J Mol Biol* **386:** 1108–1122.

Oyama, T., Ishino, S., Shirai, T., Yamagami, T., Nagata, M., Ogino, H., *et al*. (2016) Atomic structure of an archaeal GAN suggests its dual roles as an exonuclease in DNA repair and a CMG component in DNA replication. *Nucleic Acids Res* **44:** 9505–9517.

Pajares, M., Jiménez-Moreno, N., Dias, I.H., Debelec, B., Vucetic, M., Fladmark, K.E., *et al*. (2015) Redox control of protein degradation. *Redox Biol* **6:** 409–420.

Panasenko, O.M. (1997) The mechanism of the hypochlorite-induced lipid peroxidation. *Biofactors* **6:** 181–190.

Pedone, E., Bartolucci, S., and Fiorentino, G. (2004) Sensing and adapting to environmental stress: the archaeal tactic. *Front Biosci* **9:** 2909–2926.

Rajapakse, N.W., Konstantinidis, G., Evans, R.G., Nguyen-Huu, T.P., Kaye, D.M., and Head, G.A. (2014) Endothelial cationic amino acid transporter-1 overexpression blunts the effects of oxidative stress on pressor responses to behavioural stress in mice. *Clin Exp Pharmacol Physiol* **41:** 1031–1037.

Reindel, S., Schmidt, C.L., Anemuller, S., and Matzanke, B.F. (2005) Expression and regulation pattern of ferritin-like DpsA in the archaeon *Halobacterium salinarum*. *Biometals* **18:** 387–397.

Sakoh, M., Ito, K., and Akiyama, Y. (2005) Proteolytic activity of HtpX, a membrane-bound and stress-controlled protease from *Escherichia coli*. *J Biol Chem* **280:** 33305–33310.

Salo, D.C., Pacifici, R.E., Lin, S.W., Giulivi, C., and Davies, K.J. (1990) Superoxide dismutase undergoes proteolysis and fragmentation following oxidative modification and inactivation. *J Biol Chem* **265:** 11919–11927.

Schmid, A.K., Pan, M., Sharma, K., and Baliga, N.S. (2011) Two transcription factors are necessary for iron homeostasis in a salt-dwelling archaeon. *Nucleic Acids Res* **39:** 2519–2533.

Schrimpf, S.P., Weiss, M., Reiter, L., Ahrens, C.H., Jovanovic, M., Malmstrom, J., *et al*. (2009) Comparative functional analysis of the *Caenorhabditis elegans* and *Drosophila melanogaster* proteomes. *PLoS Biol* **7:** e48.

Shang, F., and Taylor, A. (2011) Ubiquitin-proteasome pathway and cellular responses to oxidative stress. *Free Radic Biol Med* **51:** 5–16.

Shih, C.J., and Lai, M.C. (2010) Differentially expressed genes after hyper- and hypo-salt stress in the halophilic archaeon *Methanohalophilus portucalensis*. *Can J Microbiol* **56:** 295–307.

Shimohata, N., Chiba, S., Saikawa, N., Ito, K., and Akiyama, Y. (2002) The Cpx stress response system of *Escherichia coli* senses plasma membrane proteins and controls HtpX, a membrane protease with a cytosolic active site. *Genes Cells* **7:** 653–662.

Shukla, H.D. (2006) Proteomic analysis of acidic chaperones, and stress proteins in extreme halophile *Halobacterium* NRC-1: a comparative proteomic approach to study heat shock response. *Proteome Sci* **4:** 6.

Sips, H.J., and Hamers, M.N. (1981) Mechanism of the bactericidal action of myeloperoxidase: increased permeability of the *Escherichia coli* cell envelope. *Infect Immun* **31:** 11–16.

Southern, E.M. (1975) Detection of specific sequences among DNA fragments separated by gel electrophoresis. *J Mol Biol* **98:** 503–517.

Strahl, H., and Greie, J.C. (2008) The extremely halophilic archaeon *Halobacterium salinarum* R1 responds to potassium limitation by expression of the K+-transporting KdpFABC P-type ATPase and by a decrease in intracellular K+. *Extremophiles* **12:** 741–752.

Takehara, Y., Yamaoka, K., Sato, E.F., Yoshioka, T., and Utsumi, K. (1994) DNA damage by various forms of active oxygens and its inhibition by different scavengers using plasmid DNA. *Physiol Chem Phys Med NMR* **26:** 215–226.

Tebbe, A., Schmidt, A., Konstantinidis, K., Falb, M., Bisle, B., Klein, C., *et al*. (2009) Life-style changes of a halophilic archaeon analyzed by quantitative proteomics. *Proteomics* **9:** 3843–3855.

The UniProt Consortium. (2017) UniProt: the universal protein knowledgebase. *Nucleic Acids Res* **45:** D158–D169.

Thompson, D.M., Lu, C., Green, P.J., and Parker, R. (2008) tRNA cleavage is a conserved response to oxidative stress in eukaryotes. *RNA* **14:** 2095–2103.

Van, P.T., Schmid, A.K., King, N.L., Kaur, A., Pan, M., Whitehead, K., *et al*. (2008) *Halobacterium salinarum* NRC-1 PeptideAtlas: toward strategies for targeted proteomics and improved proteome coverage. *J Proteome Res* **7:** 3755–3764.

Van Hoof, D., Pinkse, M.W.H., Oostwaard, D.W.-V., Mummery, C.L., Heck, A.J.R., and Krijgsveld, J. (2007) An experimental correction for arginine-to-proline conversion artifacts in SILAC-based quantitative proteomics. *Nat Methods* **4:** 677–678.

Vizcaino, J.A., Csordas, A., del-Toro, N., Dianes, J.A., Griss, J., Lavidas, I., *et al*. (2016) 2016 update of the PRIDE database and its related tools. *Nucleic Acids Res* **44:** D447–D456.

Wang, G. (2016) Chloride flux in phagocytes. *Immunol Rev* **273:** 219–231.

Weist, S., Eravci, M., Broedel, O., Fuxius, S., Eravci, S., and Baumgartner, A. (2008) Results and reliability of protein quantification for two-dimensional gel electrophoresis strongly depend on the type of protein sample and the method employed. *Proteomics* **8:** 3389–3396.

Wendoloski, D., Ferrer, C., and Dyall-Smith, M.L. (2001) A new simvastatin (mevinolin)-resistance marker from *Haloarcula hispanica* and a new *Haloferax volcanii* strain cured of plasmid pHV2. *Microbiology* **147:** 959–964.

Whitehead, K., Kish, A., Pan, M., Kaur, A., Reiss, D.J., King, N., *et al*. (2006) An integrated systems approach for understanding cellular responses to gamma radiation. *Mol Syst Biol* **2:** 47.

Wichgers Schreur, P.J., Rebel, J.M., Smits, M.A., van Putten, J.P., and Smith, H.E. (2011) TroA of *Streptococcus suis* is required for manganese acquisition and full virulence. *J Bacteriol* **193:** 5073–5080.

Williams, T.J., Lauro, F.M., Ertan, H., Burg, D.W., Poljak, A., Raftery, M.J., and Cavicchioli, R. (2011) Defining the response of a microorganism to temperatures that span its complete growth temperature range (–2°C to 28°C) using multiplex quantitative proteomics. *Environ Microbiol* **13:** 2186–2203.

Williams, T.J., Liao, Y., Ye, J., Kuchel, R.P., Poljak, A., Raftery, M.J., and Cavicchioli, R. (2017) Cold adaptation of the Antarctic haloarchaea *Halohasta litchfieldiae* and *Halorubrum lacusprofundi*. *Environ Microbiol* **19:** 2210–2227.

Wong, K.S., Bhandari, V., Janga, S.C., and Houry, W.A. (2017) The RavA-ViaA chaperone-like system interacts with and modulates the activity of the fumarate reductase respiratory complex. *J Mol Biol* **429:** 324–344.

Woodman, I.L., Brammer, K., and Bolt, E.L. (2011) Physical interaction between archaeal DNA repair helicase Hel308 and replication protein A (RPA). *DNA Repair (Amst)* **10:** 306–313.

Xia, Q., Hendrickson, E.L., Zhang, Y., Wang, T., Taub, F., Moore, B.C., *et al*. (2006) Quantitative proteomics of the archaeon *Methanococcus maripaludis* validated by microarray analysis and real time PCR. *Mol Cell Proteomics* **5:** 868–881.

Yi, G.S., Song, Y., Wang, W.W., Chen, J.N., Deng, W., Cao, W., *et al*. (2017) Two archaeal RecJ nucleases from *Methanocaldococcus jannaschii* show reverse hydrolysis polarity: implication to their unique function in archaea. *Genes (Basel)* **8:** pii: E211.

Zeth, K., Offermann, S., Essen, L.O., and Oesterhelt, D. (2004) Iron-oxo clusters biomineralizing on protein surfaces: structural analysis of *Halobacterium salinarum* DpsA in its low- and high-iron states. *Proc Natl Acad Sci USA* **101:** 13780–13785.

Zhou, G., Kowalczyk, D., Humbard, M.A., Rohatgi, S., and Maupin-Furlow, J.A. (2008) Proteasomal components required for cell growth and stress responses in the haloarchaeon *Haloferax volcanii*. *J Bacteriol* **190:** 8096–8105.

Zhu, M., Simons, B., Zhu, N., Oppenheimer, D.G., and Chen, S. (2010) Analysis of abscisic acid responsive proteins in *Brassica napus* guard cells by multiplexed isobaric tagging. *J Proteomics* **73:** 790–805.

Supporting information

Additional Supporting Information may be found in the online version of this article at the publisher's web-site:

Table S1. Peptide modification dataset used to calculate heavy proline conversion from heavy arginine.

Table S2. *Haloferax volcanii* 2565 proteins identified across all four replicates and 1806 proteins identified in all four replicates at a *q*-value of 0.01 or less.

Table S3. 50 most abundant proteins of *Haloferax volcanii* identified by SILAC analysis.

Table S4. 50 least abundant proteins of *Haloferax volcanii* identified by SILAC analysis.

Table S5. Statistical analysis of label-swap replication of SILAC experiments to examine the effect of labelling on protein abundance.

Table S6. *Haloferax volcanii* proteins of differential abundance by NaOCl treatment at a *p*-value less than 0.05.

Table S7. *Haloferax volcanii* proteins up at least 1.5-fold by NaOCl treatment at a *p*-value less than 0.05.

Table S8. *Haloferax volcanii* proteins down at least 1.5-fold by NaOCl treatment at a *p*-value less than 0.05.